Journal of Applied Mathematics and Physics (ZAMP)
Vol. 37, January 1986

0044-2275/86/001064-14 $ 4.30/0

The axial displacement of a disc inclusion embedded in a penny-shaped crack

By A. P. S. Selvadurai and B. M. Singh, Dept. of Civil Engineering, Carleton University, Ottawa, Ontario, Canada K1S 5B6

1. Introduction

The category of three-dimensional problems which deal with elastic media which are reinforced with inclusions is of interest to the study of composite materials. Comprehensive expositions of inclusion problems in classical elasticity theory are given by Mura [1], Willis [2] and Walpole [3]. The flat disc shaped inclusion problems form a limiting case of the general class of three-dimensional ellipsoidal or spheroidal inclusion problems. The disc inclusion problem in classical elasticity has also received concerted attention. An extensive review of this category of inclusion problem will be given in a forthcoming article by Selvadurai [4].

This particular paper focusses attention on the interaction between a penny-shaped rigid inclusion and a penny-shaped crack which itself may be created by the wedging action of the inclusion. The stress analysis of the interaction of cracks and inclusions is of particular interest to the study of thermally and environmentally induced degradation of multiphase composites. Recently, Selvadurai and Singh [5] have examined the problem of the internal indentation of a penny-shaped crack by a smooth rigid penny-shaped inclusion of finite thickness (Fig. 1). By employing a Hankel transform development of the governing

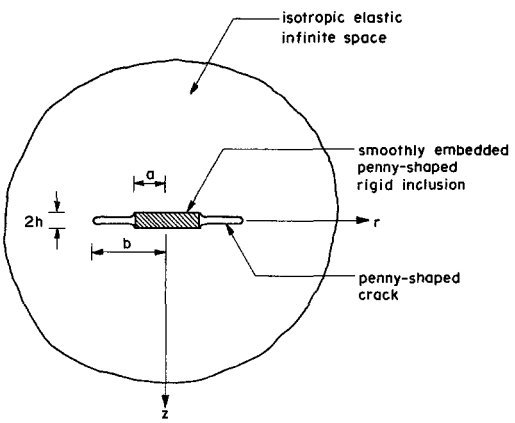

Figure 1
Penny-shaped rigid inclusion wedged in smooth contact in a penny-shaped crack.

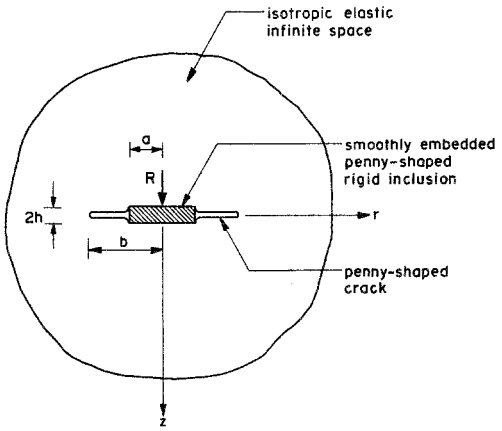

Figure 2
Axial loading of the penny-shaped rigid inclusion wedged in a penny-shaped crack.

equations, the mixed boundary value problem is reduced to the solution of a system of triple integral equations. These integral equations are further reduced to a single Fredholm integral equation of the second kind, which is solved in an approximate fashion. The approximate method involved the expansion of the governing function in a power series in terms of a small non-dimensional parameter. The small parameter is taken as the ratio of the radius of the penny-shaped inclusion to the radius of the penny-shaped crack. The numerical analysis yields a corresponding series expansion solution for the stress intensity factor at the boundary of the penny-shaped crack due to the wedging action of the smoothly embedded rigid inclusion. The present paper extends the above study to include direct axisymmetric loading of the wedged inclusion by a central force (Fig. 2). The directly loaded inclusion problem provides a useful auxiliary solution which can be used in conjunction with Betti's reciprocal theorem to study the interaction between the smoothly embedded inclusion and externally applied loads. The mixed boundary value problem associated with the directly loaded smoothly wedged inclusion is formulated via a Hankel transform development of the governing equations. The resulting integral equations are solved in an exact fashion. Finally, exact closed form results are derived for the axial stiffness of the inclusion and the stress intensity factor at the boundary of the penny-shaped crack.

2. Fundamental equations

For the analysis of the axisymmetric problem related to both symmetric and asymmetric identation of the penny-shaped crack by the rigid penny-shaped inclusion, we employ the strain potential function approach of Love [6]. Briefly, the solution of the displacement equations of equilibrium, for a medium free of body forces, can be represented in terms of a bi-harmonic function $\Phi(r, z)$, i.e.,

$$\nabla^2 \nabla^2 \Phi(r, z) = 0 \tag{1}$$

where

$$\nabla^2 = \frac{\partial^2}{\partial r^2} + \frac{1}{r}\frac{\partial}{\partial r} + \frac{\partial^2}{\partial z^2} \tag{2}$$

is the axisymmetric form of Laplace's operator referred to the cylindrical polar coordinate system. The components of the displacement vector $\boldsymbol{u}$ and the Cauchy stress tensor $\boldsymbol{\sigma}$ referred to the cylindrical polar coordinate system can be expressed in terms of the derivatives of Φ. We have

$$2G u_r = -\frac{\partial^2 \Phi}{\partial r \partial z} \tag{3}$$

$$2G u_z = 2(1-\nu)\nabla^2 \Phi - \frac{\partial^2 \Phi}{\partial z^2} \tag{4}$$

where G and ν are the linear elastic shear modulus and Poisson's ratio respectively. Similarly, the components of the stress tensor are given by

$$\sigma_{rr} = \frac{\partial}{\partial z}\left\{\nu\nabla^2 - \frac{\partial^2}{\partial z^2}\right\}\Phi \tag{5}$$

$$\sigma_{\theta\theta} = \frac{\partial}{\partial z}\left\{\nu\nabla^2 - \frac{1}{r}\frac{\partial}{\partial r}\right\}\Phi \tag{6}$$

$$\sigma_{zz} = \frac{\partial}{\partial z}\left\{(2-\nu)\nabla^2 - \frac{\partial^2}{\partial z^2}\right\}\Phi \tag{7}$$

$$\sigma_{rz} = \frac{\partial}{\partial r}\left\{(1-\nu)\nabla^2 - \frac{\partial^2}{\partial z^2}\right\}\Phi \tag{8}$$

3. Symmetric indentation of the penny shaped crack

A complete analysis of the problem of the symmetric internal indentation of a penny-shaped crack by a smoothly embedded rigid penny-shaped inclusion (of thickness 2 h), was given by Selvadurai and Singh [5]. In view of the importance of this problem to the physical basis of the asymmetric indentation problem that will be discussed in the ensuing section, we shall present here a brief summary of the salient results. Since the internal indentation is symmetric about $z = 0$, attention can be restricted to the examination of a reduced mixed boundary value problem associated with a single halfspace region occupying $z \geqq 0$. The mixed boundary conditions associated with the smooth indentation of the

penny-shaped crack are as follows:

$$u_z(r, 0) = h; \qquad 0 \leqq r \leqq a \tag{9}$$

$$u_z(r, 0) = 0; \qquad b \leqq r < \infty \tag{10}$$

$$\sigma_{zz}(r, 0) = 0; \qquad a < r < b \tag{11}$$

$$\sigma_{rz}(r, 0) = 0; \qquad 0 \leqq r < \infty \tag{12}$$

For the integral equation formulation of the mixed boundary value problem posed by (9)–(12), we seek solutions of (1) which can be obtained by a Hankel transform development of the same. Also, the displacement and stress fields derived from $\Phi(r, z)$ should reduce to zero as $(r^2 + z^2)^{1/2} \to \infty$. Following Sneddon [7], the relevant solution is given by

$$\Phi(r, z) = \int_0^\infty \xi \{A(\xi) + z B(\xi)\} e^{-\xi z} J_0(\xi r) \, d\xi \tag{13}$$

where $A(\xi)$ and $B(\xi)$ are unknown functions. Using (13) and (3)–(8), the mixed boundary conditions (9)–(12) yield the following system of triple integral equations for a single unknown function $R(\xi)$ (the functions $A(\xi)$ and $B(\xi)$ can be expressed in terms of $R(\xi)$):

$$H_0\{\xi^{-2} R(\xi); r\} = h^*; \qquad 0 \leqq r \leqq a \tag{14}$$

$$H_0\{\xi^{-1} R(\xi); r\} = 0; \qquad a < r < b \tag{15}$$

$$H_0\{\xi^{-2} R(\xi); r\} = 0; \qquad b \leqq r < \infty \tag{16}$$

where $h^* = -h G/(1 - \nu)$ and H_n ($n = 0, 1$ etc.) is the Hankel operator of order n which is defined by

$$H_n\{f(\xi); r\} = \int_0^\infty \xi f(\xi) J_n(\xi r) \, d\xi . \tag{17}$$

The method employed by Selvadurai and Singh [5] for the solution of the triple system (14)–(16) follows in general the approximate procedures developed by Cooke [8]. Briefly, by assuming that (15) admits the representation

$$H_0\{\xi^{-1} R(\xi); r\} = \begin{cases} g_1(r); & 0 < r < a \quad (18) \\ g_2(r); & b < r < \infty \quad (19) \end{cases}$$

we can reduce the triple system (14)–(16) effectively to the solution of a single Fredholm integral equation of the second kind

$$\psi(\eta_1) = 1 + \int_0^1 \psi(\xi_1) K(\xi_1, \eta_1) \, d\xi_1; \qquad 0 \leqq \eta_1 \leqq 1 \tag{20}$$

where

$$\psi(\eta_1) = \frac{\pi a}{2h^*}(1-\eta_1^2)^{1/2}\, g_1(a\eta_1) \tag{21}$$

$$\xi = \xi_1 a; \qquad \eta = \eta_1 a \tag{22}$$

$$K(\xi_1, \eta_1) = \frac{4c\,\xi_1(1-c^2\xi_1^2)^{1/2}}{\pi^2(1-\xi_1^2)^{1/2}} \int_1^\infty F(\xi_1, \eta_1, t)\,\mathrm{d}t \tag{23}$$

$$F(\xi_1, \eta_1, t) = \frac{\left\{1-\dfrac{c^2}{t_1^2}\right\}^{1/2}}{t_1^3\left\{1-\dfrac{1}{t_1^2}\right\}^{1/2}\left\{1-\dfrac{c^2\xi_1^2}{t_1^2}\right\}\left\{1-\dfrac{c^2\eta_1^2}{t_1^2}\right\}} \tag{24}$$

and $c = a/b$. The Fredholm integral equation of the second-kind given by (20) can be solved by employing several numerical schemes (see e.g. Atkinson [9], Baker [10]). The method employed in [5] focusses on the development of a power series solution for $\psi(\eta_1)$ where the expansion parameter is c. We assume that the function $\psi(\eta_1)$ can be expressed in the form

$$\psi(\eta_1) = \sum_{i=0}^{N} c^i \psi_i(\eta_1). \tag{25}$$

The kernel function $K(\xi_1, \eta_1)$ can also be expanded in power series in c; by substituting the resulting expressions in (20), performing the integrations and comparing terms of order c^i $(i = 0, 1, 2, \ldots, 6)$ we obtain the series solution for $\psi(\eta_1)$.

The results of primary interest to the present paper are the force resultants on the faces of the indenting inclusion and the flaw opening mode stress intensity factor at the boundary of the penny-shaped crack. These results can also be evaluated in power series form. The force on the plane face of the smoothly wedged inclusion is given by

$$P = \frac{\pi h G a}{(1-\nu)}\left\{\frac{4}{\pi} + \frac{16}{\pi^3}c + \frac{64}{\pi^5}c^2 + c^3\left(\frac{32}{9\pi^3} + \frac{256}{\pi^7}\right) + c^4\left(\frac{256}{9\pi^5} + \frac{1024}{\pi^9}\right) + c^5\left(\frac{368}{225\pi^3} + \frac{512}{3\pi^7} + \frac{4096}{\pi^{11}}\right) + 0(c^6)\right\}. \tag{26}$$

Similarly, the flaw opening mode stress intensity factor at the boundary of the penny-shaped crack is given by

$$K_1 = \frac{hG}{\pi(1-\nu)\sqrt{b}}\left\{\frac{4c}{\pi} + \frac{16}{\pi^3}c^2 + c^3\left(\frac{64}{\pi^5} + \frac{4}{3\pi}\right) + c^4\left(\frac{80}{9\pi^3} + \frac{256}{\pi^7}\right) + c^5\left(\frac{448}{9\pi^5} + \frac{1024}{\pi^9} + \frac{4}{5\pi}\right) + 0(c^6)\right\}. \tag{27}$$

From the discussion presented here it is evident that the wedging action of the smoothly embedded rigid penny-shaped inclusion induces an appropriate dipole of forces at the faces of the crack and the magnitude of each force is given by (26). Consequently, when the smoothly embedded inclusion is subjected to a resultant axial force R (Fig. 2), we can expect the contact between the surfaces of the penny-shaped crack and the smoothly embedded inclusion to be maintained provided $(R/2) < P$.

4. Axial loading of the smoothly embedded inclusion

We now examine the problem of the axial loading of a penny-shaped rigid circular inclusion of thickness $2h$ and radius a which is wedged in smooth contact in a penny-shaped crack of radius b (Fig. 2). Since the axisymmetric state of deformation exhibits a state of asymmetry about the plane $z = 0$, we can restrict the attention to the analysis of a single halfspace region $z \geqq 0$. The plane $z = 0$ is subjected to the following mixed boundary condition.

$$u_z(r, 0) = \Delta; \qquad 0 \leqq r \leqq a \tag{28}$$

$$u_r(r, 0) = 0; \qquad b \leqq r < \infty \tag{29}$$

$$\sigma_{zz}(r, 0) = 0; \qquad a < r < \infty \tag{30}$$

$$\sigma_{rz}(r, 0) = 0; \qquad 0 < r < b. \tag{31}$$

Using the solution of (1) given by (13) and the expressions (3)–(8), these mixed boundary conditions can be reduced to the following system of integral equations

$$H_0[\xi\{\xi A(\xi) + 2(1-2\nu) B(\xi)\}; r] = -2G\Delta; \qquad 0 \leqq r \leqq a \tag{32}$$

$$H_1[\xi\{-\xi A(\xi) + B(\xi)\}; r] = 0; \qquad b \leqq r < \infty \tag{33}$$

$$H_0[\xi^2\{\xi A(\xi) + (1-2\nu) B(\xi)\}; r] = 0; \qquad a < r < \infty \tag{34}$$

$$H_1[\xi^2\{\xi A(\xi) - 2\nu B(\xi)\}; r] = 0; \qquad 0 < r < b. \tag{35}$$

We now make the assumption that as $b \to \infty$, we should recover, from the solution developed, the appropriate results for the problem of the indentation of a halfspace region by a smooth rigid punch. It is convenient to introduce two auxiliary functions $M(\xi)$ and $N(\xi)$ such that

$$A(\xi) = \frac{1}{\xi^3}\{(1-2\nu) N(\xi) + 2\nu M(\xi)\} \tag{36}$$

$$B(\xi) = \frac{1}{\xi^3}\{M(\xi) - N(\xi)\}. \tag{37}$$

Using the substitutions (36) and (37), the integral equations (32)–(35) can be written as

$$H_0\left[\xi^{-1}\left\{M(\xi)-\frac{(1-2\nu)}{(2-2\nu)}N(\xi)\right\};r\right]=-\frac{G\Delta}{(1-\nu)};\qquad 0\leqq r\leqq a \tag{38}$$

$$H_1\left[\xi^{-1}\left\{\frac{(1-2\nu)}{(2-2\nu)}M(\xi)-N(\xi)\right\};r\right]=0;\qquad b\leqq r<\infty \tag{39}$$

$$H_0[M(\xi);r]=0;\qquad a<r<\infty \tag{40}$$

$$H_1[N(\xi);r]=0;\qquad 0<r<b \tag{41}$$

For the solution of the system of integral Eqs. (38)–(40) we assume that (40) and (41) admit the following representations in $r\,\varepsilon\,(0,a)$ and $r\,\varepsilon\,(b,\infty)$ respectively: i.e.,

$$H_0[M(\xi);r]=f_1(r);\qquad 0<r<a \tag{42}$$

$$H_1[N(\xi);r]=f_2(r);\qquad b<r<\infty \tag{43}$$

where $f_1(r)$ and $f_2(r)$ are unknown functions. By making use of the Hankel inversion theorem we obtain from (40) and (42) the following:

$$M(\xi)=\int_0^a u f_1(u) J_0(\xi u)\,\mathrm{d}u. \tag{44}$$

Similarly, from (41) and (43) we obtain

$$N(\xi)=\int_b^\infty u f_2(u) J_1(\xi u)\,\mathrm{d}u. \tag{45}$$

By substituting (44) and (45) into (38) and (39), we obtain the following system of coupled integral equations for the functions $f_i(r)$, $(i=1,2)$:

$$\int_0^a u f_1(u) K(u,r)\,\mathrm{d}u-\frac{(1-2\nu)}{(2-2\nu)}\int_b^\infty f_2(r)\,\mathrm{d}r=-\frac{G\Delta}{(1-\nu)};\qquad 0<r<a \tag{46}$$

$$\frac{(1-2\nu)}{(2-2\nu)r}\int_0^a u f_1(u)\,\mathrm{d}u-\int_b^\infty u f_2(u) L(u,r)\,\mathrm{d}u=0;\qquad b<r<\infty \tag{47}$$

where

$$K(u,r)=\int_0^\infty J_0(\xi r) J_0(\xi u)\,\mathrm{d}\xi \tag{48}$$

$$L(u,r)=\int_0^\infty J_1(\xi u) J_1(\xi r)\,\mathrm{d}\xi. \tag{49}$$

In obtaining (46) and (47) we make use of the following integrals (see e.g. Erdelyi et al. [11])

$$\int_0^\infty J_1(\xi\alpha)\, J_0(\xi\beta)\, d\xi = \begin{cases} \dfrac{1}{\alpha}; & \beta < \alpha \\ 0; & \beta > \alpha . \end{cases} \tag{50}$$

The kernel functions (48) and (49) can be expressed in the form

$$K(u,r) = \frac{2}{\pi} \int_0^{\min(u,r)} \frac{ds}{[(u^2 - s^2)(r^2 - s^2)]^{1/2}} \tag{51}$$

$$L(u,r) = \frac{2ru}{\pi} \int_{\max(u,r)}^\infty \frac{ds}{s^2 [(s^2 - r^2)(s^2 - u^2)]^{1/2}} \tag{52}$$

where $\min(u,r)$ and $\max(u,r)$ denote the minimum and maximum values of u and r respectively. With the aid of (51), the integral Eq. (46) can be reduced to the following Abel type integral equation

$$\int_0^r \frac{ds}{(r^2 - s^2)^{1/2}} \int_s^a \frac{u f_1(u)\, du}{(u^2 - s^2)^{1/2}} = \frac{\pi(1-2\nu)}{4(1-\nu)} \int_b^\infty f_2(r)\, dr - \frac{G\Delta\pi}{2(1-\nu)}; \quad 0 < r < a . \tag{53}$$

The solution of (53) can be written as

$$f_1(u) = \frac{(1-2\nu)}{\pi(1-\nu)(a^2 - u^2)^{1/2}} \int_b^\infty f_2(r)\, dr - \frac{2G\Delta}{\pi(1-\nu)(a^2 - u^2)^{1/2}}; \; 0 < u < a . \tag{54}$$

In a similar manner by making use of (52), we can reduce (47) to the following Abel type integral equation

$$\int_r^\infty \frac{ds}{s^2 (s^2 - r^2)^{1/2}} \int_b^s \frac{u^2 f_2(u)\, du}{(s^2 - u^2)^{1/2}} = \frac{\pi(1-2\nu)}{4(1-\nu) r^2} \int_0^a u f_1(u)\, du; \quad b < r < \infty . \tag{55}$$

The solution of (55) can be written as

$$\frac{1}{s^2} \int_b^s \frac{u^2 f_2(u)\, du}{(s^2 - u^2)^{1/2}} = -\frac{(1-2\nu)}{(2-2\nu)} \int_0^a u f_1(u)\, du \left\{ \frac{d}{ds} \int_s^\infty \frac{dr}{r(r^2 - s^2)^{1/2}} \right\}; \; b < s < \infty . \tag{56}$$

Since

$$\frac{d}{ds} \int_s^\infty \frac{dr}{r(r^2 - s^2)^{1/2}} = -\frac{\pi}{2s^2} \tag{57}$$

the result (56) can be simplified and inverted to give the following:

$$f_2(u) = \frac{(1-2\nu)}{2u(1-\nu)(u^2 - b^2)^{1/2}} \int_0^a v f_1(v)\, dv_1; \qquad b < u < \infty . \tag{58}$$

By substituting the value of $f_1(u)$ given by (54) we find that

$$f_2(u) = \frac{(1-2\nu)^2 a C^*}{2\pi(1-\nu)^2 u(u^2-b^2)^{1/2}} - \frac{(1-2\nu) G \Delta a}{(1-\nu)^2 \pi u (u^2-b^2)^{1/2}}; \quad b < u < \infty \tag{59}$$

where

$$C^* = \int_b^\infty f_2(u)\, du. \tag{60}$$

Integrating the Eq. (59) between the limits b to ∞ it can be shown that

$$C^* = -\frac{2 G \Delta c (1-2\nu)}{\{4(1-\nu)^2 - c(1-2\nu)^2\}}. \tag{61}$$

This formally completes the solution of the system of integral Eqs. (32)–(35). The explicit expression for f_2 is given by (59) and the expression for f_1 takes the form

$$f_1(u) = \frac{(1-2\nu) C^*}{\pi(1-\nu)(a^2-u^2)^{1/2}} - \frac{2 G \Delta}{\pi(1-\nu)(a^2-u^2)^{1/2}}; \quad 0 < u < a. \tag{62}$$

These solutions are sufficient for the purposes of evaluation of the axial stiffness of the inclusion and the stress intensity factor at the boundary of the penny-shaped crack.

5. Load-displacement relationship for the smoothly embedded inclusion and the stress intensity factor at the boundary of the crack

Results of engineering interest concerns the axial load-displacement relationship for the penny-shaped rigid inclusion wedged in smooth contact in a penny-shaped crack and the flaw shearing mode stress intensity factor K_2 at the boundary of the penny-shaped crack.

The load-displacement relationship for the smoothly wedged penny-shaped inclusion is given by

$$R = -2\pi \int_0^a \{\sigma_{zz}(r, 0^+) - \sigma_{zz}(r, 0^-)\}\, r\, dr \tag{63}$$

where the positive and negative superscripts refer to the faces of the inclusion in contact with the halfspace regions $z \geqq 0$ and $z \leqq 0$ respectively. Making use of the results (40), (44) and (62) and noting that $\sigma_{zz}(r, 0^-) = -\sigma_{zz}(r, 0^+)$, (63) can be reduced to the form

$$R = -4\pi \int_0^a f_1(r) r\, dr. \tag{64}$$

Using (62) in (64) we obtain the following load-displacement relationship:

$$R = \frac{8\,G\,\Delta\,a}{(1-\nu)}\left[1 + \frac{c(1-2\nu)^2}{\{4(1-\nu)^2 - c(1-2\nu)^2\}}\right]. \tag{65}$$

The flaw shearing or mode 2 stress intensity factor at the boundary of the penny-shaped crack is defined by

$$K_2 = \lim_{r \to b^+} \{2(r-b)\}^{1/2}\,\sigma_{rz}(r,0). \tag{66}$$

Making use of the results (41) and (45), (66) can be reduced to the form

$$K_2 = \lim_{r \to b^+} \{2(r-b)\}^{1/2}\,f_2(r). \tag{67}$$

Making use of (59), (67) yields the following

$$K_2 = -\frac{G\,\Delta\,a(1-2\nu)}{\pi(1-\nu)^2\,b^{3/2}}\left[1 + \frac{c(1-2\nu)^2}{\{4(1-\nu)^2 - c(1-2\nu)^2\}}\right]. \tag{68}$$

6. Limiting cases and numerical results

In this section we shall present certain numerical results which will illustrate the manner in which the axial stiffness of the wedged penny-shaped inclusion and the stress intensity factor at the boundary of the penny-shaped crack are influenced by the inclusion/crack radii ratio (c) and Poisson's ratio of the elastic material. Prior to performing any numerical evaluations, it is instructive to establish the accuracy of the exact solutions (65) and (68) in predicting exact solutions to certain limiting cases.

In the limiting case when the radius of the penny-shaped crack becomes infinite (i.e. $c \to 0$), the asymmetric indentation problem reduces to the problem of the axial loading of a rigid inclusion wedged in smooth contact at two separate halfspace regions (Fig. 3a). Using classical results [12] for the indentation of a halfspace by a smooth circular punch of radius a it can be shown that

$$R = \frac{8\,G\,\Delta\,a}{(1-\nu)}. \tag{69}$$

This is in agreement with the result obtained from (65) as $c \to 0$.

In the limit of material incompressibility, we note that both (65) and (69) reduce to the single result

$$R = 16\,G\,\Delta\,a. \tag{70}$$

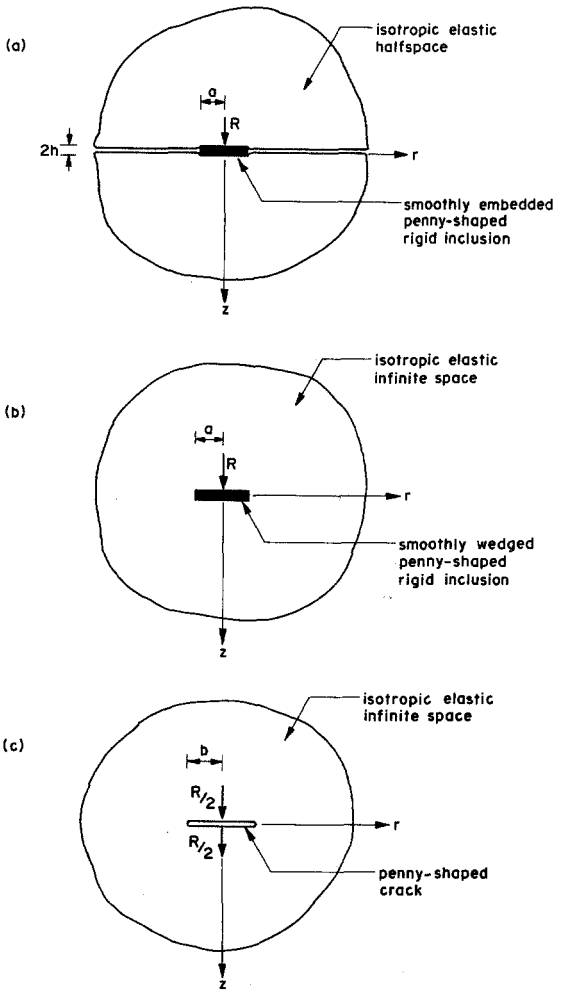

Figure 3
Direct loading of a penny-shaped rigid inclusion embedded in a penny-shaped crack. Limiting cases.

Since, in the limit of material incompressibility the result for the axial stiffness of the inclusion wedged in the crack coincides with the equivalent result for the inclusion wedged between two halfspace regions it is evident that when $\nu = \frac{1}{2}$ the geometry of the penny-shaped crack has no influence on the axial stiffness.

In the special case when $c = 1$, the result (65) gives the solution for the axial stiffness of a disc inclusion wedged in smooth contact in a crack of equal radius. The corresponding result for this somewhat artificial problem is

$$R = \frac{32\, G\, \Delta a (1 - \nu)}{(3 - 4\nu)}. \tag{71}$$

It is of interest to note that the Eq. (71) is identical to the result obtain by Collins [13], Kanwal and Sharma [14] and Selvadurai [15] for the axial displacement of a penny-shaped rigid inclusion embedded in bonded contact in an elastic solid.

The accuracy of the result (68) for the stress intensity factor at the boundary of the penny-shaped crack can be established by invoking the following limiting procedure. In the special case when $a \to 0$, the geometry of the inclusion approaches that of a concentrated force, of magnitude $R^* = 4G\Delta a/(1-\nu)$, acting at the centre of the penny-shaped crack surface $(0, 0^+)$. Owing to the asymmetry of the deformation, the location $(0, 0^-)$ is also subjected to an equal and opposite force R^*. The action of this dipole of asymmetric forces (Fig. 3b) gives the following stress intensity factor

$$K_2 = -\frac{R^*(1-2\nu)}{4(1-\nu)\pi b^{3/2}}\left[1 + \frac{c(1-2\nu)^2}{\{4(1-\nu)^2 - c(1-2\nu)^2\}}\right]. \tag{72}$$

As $a \to 0, c \to 0$ and the expression (72) reduces to the result given by Kassir and Sih [16] for the flaw shearing mode stress intensity factor at the boundary of a penny-shaped crack loaded by an asymmetric dipole of forces. It may also be noted that in the limit of material incompressibility, the shear stresses on the plane $z = 0$ vanishes; consequently $K_2 \equiv 0$. The Fig. 4 illustrates the manner in which the non-dimensional axial stiffness $(\bar{R})$ of the rigid disc inclusion wedged in the penny-shaped crack, given by

$$\frac{R(1-\nu)}{8G\Delta a} = \bar{R}(c, \nu) \tag{73}$$

is influenced by the Poisson's ratio of the elastic medium and the radii ratio of the penny-shaped rigid inclusion to the penny-shaped crack. The Fig. 5 illustrates the manner in which the normalized stress intensity factor $\bar{K}_2$ given by

$$-\frac{\pi(1-\nu)K_2 b^{3/2}}{G\Delta a(1-2\nu)} = \bar{K}_2(c, \nu) \tag{74}$$

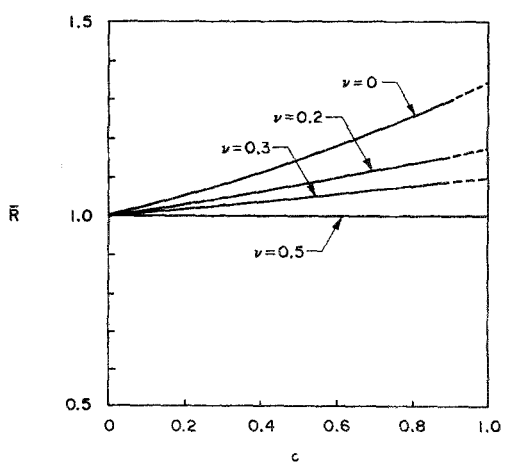

Figure 4
Non-dimensional axial stiffness of a penny-shaped rigid inclusion wedged in a penny-shaped crack.

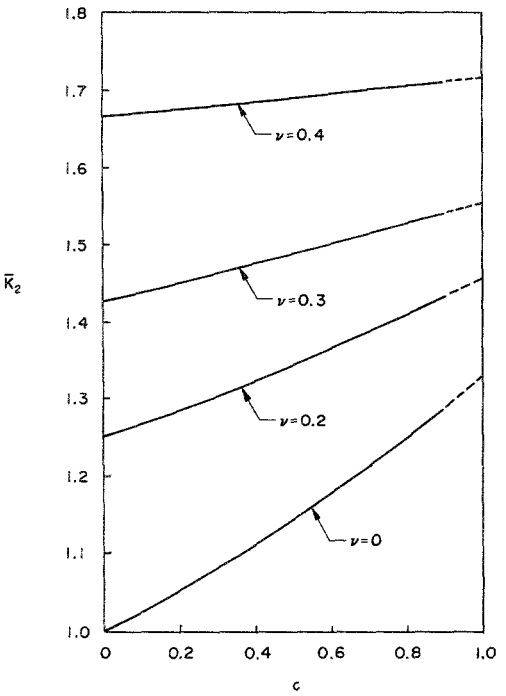

Figure 5
Normalized flow shearing mode stress intensity factor at the boundary of the penny-shaped crack due to axial loading of the wedged disc inclusion.

varies with c and ν. In both cases the results for $\bar{R}$ and $\bar{K}_2$ are presented for $\nu \in (0, 0.5)$ and $c \in (0, 0.9)$. These numerical results indicate that the axial stiffness of the wedged inclusion is reduced as $b \to \infty$. Since K_2 reduces to zero when $\nu = 0.5$, the numerical results given in Fig. 5 take into account values of $\nu \in (0, 0.4)$.

7. Conclusions

The paper considers the axial loading of a penny-shaped rigid inclusion which is wedged in smooth contact in a penny-shaped crack. The results for the axial stiffness of the inclusion and the crack shearing mode stress intensity factor at the boundary of the penny-shaped crack are evaluated in exact closed form. Owing to the assumption of smooth contact at the inclusion-crack interface the relationship for the axial stiffness of the inclusion will be valid only in the range $(R/2) < P$ where P and R are defined by Eqs. (26) and (65). Alternatively, the condition $R = 2P$ can be used to establish a limiting relationship between the wedging displacement h and the axial displacement Δ.

References

[1] T. Mura, *Micromechanics of Defects in solids,* Sijthoff and Noordhoff, The Netherlands (1981).
[2] J. F. Willis, *Variational and related methods for the overall properties of composites,* Advances in Applied Mechanics, (C.-S. Yih, Ed.) Academic Press, New York, Vol. *21,* 1–78 (1981).
[3] L. J. Walpole, *Elastic behaviour of composites materials: Theoretical foundations,* Advances in Applied Mechanics (C.-S. Yih, Ed.), Academic Press, New York, Vol. *21,* 169–242 (1981).
[4] A. P. S. Selvadurai, *Disc inclusion problems in classical elasticity* (in preparation) (1986).
[5] A. P. S. Selvadurai and B. M. Singh, *On the expansion of a penny-shaped crack by a rigid circular disc inclusion,* Int. J. Fracture *25,* 69–77 (1984).
[6] A. E. H. Love, *A treatise on the mathematical theory of elasticity,* Cambridge University Press, London 1927.
[7] I. N. Sneddon, *The use of integral transforms,* McGraw-Hill, New York 1972.
[8] J. C. Cooke, *Triple integral equations,* Quart. J. Mech. Appl. Math. *16,* 193–203 (1963).
[9] K. Atkinson, *A survey of numerical methods for the solution of Fredholm integral equations of the second-kind,* Soc. for Industrial and Appl. Math., Philadelphia, Pa. 1976.
[10] C. T. H. Baker, *The numerical treatment of integral equations,* Clarendon Press, Oxford 1977.
[11] A. Erdelyi, W. Magnus, F. Oberhettinger and F. G. Tricomi, *Tables of integral transforms,* Vols I and II, McGraw-Hill, New York 1954.
[12] G. M. L. Gladwell, *Contact problems in the classical theory of elasticity,* Sijthoff and Noordhoff, The Netherlands 1980.
[13] W. D. Collins, *Some axially symmetric stress distributions in elastic solids containing penny-shaped cracks. I. Cracks in an infinite solid and a thick plate,* Proc. Roy. Soc. Ser. A *203,* 359–386 (1962).
[14] R. P. Kanwal and D. L. Sharma, *Singularity methods for elastostatics,* J. Elasticity *6,* 405–418 (1976).
[15] A. P. S. Selvadurai, *The load-deflexion characteristics of a deep rigid anchor in an elastic medium,* Geotechnique *26,* 603–612 (1976).
[16] M. K. Kassir and G. C. Sih, *Three-dimensional crack problems: mechanics of fracture, vol. 2,* (G. C. Sih, Ed.) Noordhoff, Leyden 1975.

Abstract

The present paper examines the axisymmetric problem of the axial translation of a rigid circular disc inclusion of finite thickness which is wedged in smooth contact in a penny-shaped crack. Results for the axial stiffness of the embedded inclusion and the stress intensity factor at the boundary of the penny shaped crack are evaluated in exact closed form.

Zusammenfassung

Die vorliegende Arbeit untersucht das axisymmetrische Problem der axialen Verschiebung einer starren eingebetteten Kreisscheibe mit bestimmter Dicke, die in einer reibungslosen pfennigförmigen Spalte eingekeilt ist. Ergebnisse für die axiale Steifigkeit der eingebetteten Scheibe und der Druckintensitätsfaktor am Rande der pfennigförmigen Spalte sind als eine genaue geschlossene Lösung angegeben.

(Received: April 25, 1985)